Available online at www.sciencedirect.com

SCIENCE DIRECT®

Earth and Planetary Science Letters 231 (2005) 317–336

EPSL

www.elsevier.com/locate/epsl

Deep Pacific $CaCO_3$ compensation and glacial–interglacial atmospheric CO_2

Thomas M. Marchitto[a,*], Jean Lynch-Stieglitz[b], Sidney R. Hemming[c]

[a]*Department of Geological Sciences and Institute of Arctic and Alpine Research, University of Colorado, Boulder, CO, USA*
[b]*School of Earth and Atmospheric Sciences, Georgia Institute of Technology, Atlanta, GA, USA*
[c]*Lamont-Doherty Earth Observatory and Department of Earth and Environmental Sciences, Columbia University, Palisades, NY, USA*

Received 29 March 2004; received in revised form 23 November 2004; accepted 21 December 2004

Editor: E. Boyle

Abstract

Benthic foraminiferal $\delta^{13}C$ suggests that there was a net shift of isotopically light metabolic CO_2 from the upper ocean into the deep ocean during the last glacial period. According to the '$CaCO_3$ compensation' hypothesis, this should have caused a transient drop in deep ocean CO_3^{2-} that was eventually reversed by seafloor dissolution of $CaCO_3$. The resulting increase in whole-ocean pH may have had a significant impact on atmospheric CO_2, compounding any decrease that was due to the initial vertical CO_2 shift. The opposite hypothetically occurred during deglaciation, when CO_2 was returned to the upper ocean (and atmosphere) and deep ocean CO_3^{2-} temporarily increased, followed by excess burial of $CaCO_3$ and a drop in whole-ocean pH. The deep sea record of $CaCO_3$ preservation appears to reflect these processes, with the largest excursion during deglaciation (as expected), but various factors make quantification of deep sea paleo-CO_3^{2-} difficult. Here we reconstruct deep equatorial Pacific CO_3^{2-} over the last glacial–interglacial cycle using benthic foraminiferal Zn/Ca, which is strongly affected by saturation state during calcite precipitation. Our data are in agreement with the $CaCO_3$ compensation theory, including glacial CO_3^{2-} concentrations similar to (or slightly lower than) today, and a Termination I CO_3^{2-} peak of ~25–30 μmol kg^{-1}. The deglacial CO_3^{2-} rise precedes ice sheet melting, consistent with the timing of the atmospheric CO_2 rise. A later portion of the peak could reflect removal of CO_2 from the atmosphere–ocean system due to boreal forest regrowth. $CaCO_3$ compensation alone may explain more than one third of the atmospheric CO_2 lowering during glacial times.

Keywords: carbonate compensation; carbon dioxide; benthic foraminifera; zinc; cadmium

* Corresponding author. Tel.: +1 303 492 7739; fax: +1 303 492 6388.
E-mail addresses: tom.marchitto@colorado.edu (T.M. Marchitto), jean@eas.gatech.edu (J. Lynch-Stieglitz), sidney@ldeo.columbia.edu (S.R. Hemming).

0012-821X/$ - see front matter © 2005 Elsevier B.V. All rights reserved.
doi:10.1016/j.epsl.2004.12.024

1. Introduction

1.1. Atmospheric CO_2 and $CaCO_3$ compensation

Analysis of air trapped in Antarctic ice cores indicates that atmospheric CO_2 concentrations have varied dramatically over the past glacial–interglacial cycle [1] (Fig. 1d). During the last glacial maximum (LGM, ~21 ky cal BP), CO_2 was ~190 parts per million by volume (ppmv), compared to ~280 ppmv in the pre-industrial atmosphere [2] and >370 ppmv today [3]. All viable models proposed to explain the glacial lowering call upon a transfer of CO_2 from the atmosphere into the ocean [4].

Sea surface pCO_2 (and thus atmospheric CO_2, at equilibrium) depends on the concentration of CO_2(aq) and its solubility coefficient. Sea surface CO_2(aq) may be lowered by four main mechanisms: (i) terrestrial biomass expansion may remove CO_2 from the atmosphere–ocean system; (ii) biological productivity may draw CO_2 out of the surface ocean and export it to the deep ocean; (iii) upwelling of CO_2-rich deep waters may be reduced; and (iv) the speciation of ΣCO_2 may shift away from CO_2(aq). This last mechanism is an important part of the '$CaCO_3$ compensation' hypothesis [5]. ΣCO_2 or dissolved inorganic carbon (DIC) is represented by:

$$\Sigma CO_2 = [CO_2(aq)] \leftrightarrow [H_2CO_3] \leftrightarrow [HCO_3^-] \leftrightarrow [CO_3^{2-}] \quad (1)$$

where the concentration of H_2CO_3 is negligible. The speciation of the ΣCO_2 pool helps to maintain a charge balance with the excess of conservative cations over conservative anions in seawater, which we call the alkalinity. As the ratio of alkalinity to ΣCO_2 increases, the ΣCO_2 equilibrium shifts to the right and CO_2(aq) drops. As the ratio of alkalinity to ΣCO_2 decreases, the equilibrium shifts to the left and CO_3^{2-} drops.

$CaCO_3$ compensation [5,6] calls for a deep ocean (say, >2 km depth) drop in alkalinity:ΣCO_2 and thus CO_3^{2-} at the start of glacial time due to an addition of excess metabolic CO_2 from the upper ocean. The CO_3^{2-} drop promotes dissolution of seafloor $CaCO_3$, which raises seawater alkalinity:ΣCO_2 in a 2:1 ratio until a new steady state is reached. In the simplest case of no change in the riverine supply of alkalinity to the oceans, and no change in the global oceanic formation rate of $CaCO_3$, the steady state glacial CO_3^{2-} concentration will match its original interglacial value (conversely, a change in alkalinity supply or $CaCO_3$ production would require a deepening or shoaling of the steady state lysocline to restore balance [7]). Since the initial CO_2 addition was a simple rearrangement within the ocean, the whole ocean has a net alkalinity: ΣCO_2 (pH) gain. This gain is eventually mixed to the sea surface, lowering pCO_2. At the end of glacial time the reverse occurs: excess CO_2 is returned to the upper ocean, promoting deep sea $CaCO_3$ preservation and thereby decreasing whole ocean alkalinity:ΣCO_2 (pH) and raising pCO_2. This model assumes that changes in upper ocean CO_3^{2-} are compensated to a negligible degree because much of the upper ocean remains oversaturated with respect to calcite.

In the above scenario, the glacial shift of CO_2 from upper ocean to deep ocean could theoretically be accomplished through physical and/or biological means. These include (i) reduced ventilation of the deep ocean around Antarctica [8–11]; (ii) formation of low-nutrient Glacial North Atlantic Intermediate Water (GNAIW) at the expense of North Atlantic Deep Water (NADW) [12–14]; and (iii) more efficient organic matter export (in excess of $CaCO_3$ export) due to increased nutrient supply or iron fertilization [15–17]. In each case, the upper ocean is expected to become enriched in $\delta^{13}C$ and the deep ocean depleted. Benthic foraminiferal evidence for this is clearest in the Atlantic, where the shift is mainly attributed to the formation of GNAIW and the greater northward penetration of CO_2-rich deep Southern Ocean waters [12–14]. The North Atlantic subtropical gyre (shallower than GNAIW) was also significantly enriched in $\delta^{13}C$ [18]. The transition between GNAIW and Southern Ocean waters at ~2000 m depth was dramatic, with $\delta^{13}C$ changing by roughly 1‰ within a few hundred meters. A comparable mid-depth transition has been documented for the northern Indian Ocean [19]. Data coverage in the upper Pacific is comparatively poor, but an intermediate to mid-depth $\delta^{13}C$ gradient is generally supported [13,20–22]. In the tropical Pacific, the $\delta^{13}C$ difference between deep-dwelling planktonic foraminifera and deep ocean benthic foraminifera was also larger at the LGM [23]. Overall there is good evidence in the glacial ocean for what we will call 'CO_2 deepening.' If the deepening removed CO_2 from the surface ocean

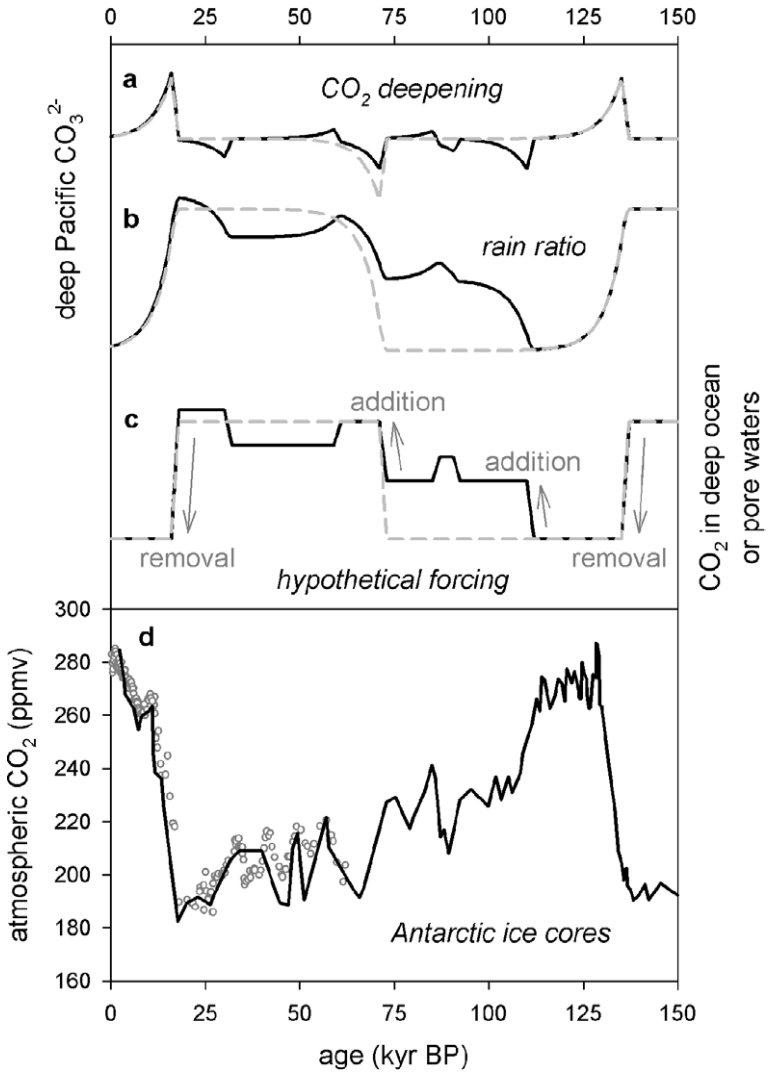

Fig. 1. Simple conceptual models for the deep Pacific CO_3^{2-} response to CO_2 deepening (a) or altering the global mean C_{org}:$CaCO_3$ rain ratio (b). The gray-dashed and black curves correspond to two levels of complexity in the hypothetical forcing, shown in (c): a simple glacial–interglacial square wave (gray dashes, after [6]) and a slightly more realistic MIS-level square wave (black). The latter is a first-order reflection of the atmospheric CO_2 history shown in (d), from the Vostok (black line, [1]) and Taylor Dome (gray circles, [80,91,92]) ice cores in Antarctica. We do not attempt to include fine-scale features such as the oscillations within MIS 3. Each shift in the forcing is spread over 2000 years, and $CaCO_3$ compensation responses reach half their steady-state magnitude ~3000 years later. No vertical scales are shown in the top panel because the magnitude of the forcing is not known a priori (see Section 5.1); increasing concentrations are up for all curves.

(rather than only intermediate depths), pCO_2 would have decreased in excess of the compensation effect.

1.2. $CaCO_3$ preservation history

If CO_2 deepening and $CaCO_3$ compensation did occur during the last glaciation, we would expect to see $CaCO_3$ dissolution and preservation events recorded in deep sea sediments. Box models suggest that each CO_3^{2-} excursion would last on the order of several thousand years before returning to a steady state that is close to the initial condition [5,7]. Since the climatic progression from the Marine Isotope Stage (MIS) 5e interglacial toward the LGM was

stepwise, we predict that the resulting negative CO_3^{2-} excursions would have been small compared to the deglacial (Termination I) positive excursion (Fig. 1a). Thus the largest signal that we expect to see in deep sea sediments is a deglacial $CaCO_3$ preservation spike.

However, other perturbations to the global carbon cycle are expected to largest during deglaciation, and these also may affect deep sea $CaCO_3$ preservation through compensation. Boreal forest regrowth following ice sheet melting removed perhaps 500 Gt of carbon, or more, from the whole ocean [24–26]. Additional CO_2 may have been removed through burial on newly submerged continental shelves [27]. Both would have contributed to deep ocean positive CO_3^{2-} excursions. Excess alkalinity may have also been removed to shelves via coral reef regrowth [28] and neritic $CaCO_3$ accumulation [29]. These would have caused negative CO_3^{2-} excursions. Fortunately all of these processes are linked to ice melting and sea level rise, and thus occur relatively late within the deglaciation or even well into the Holocene (though see terrestrial carbon caveat at end of Section 5.1). Much of the atmospheric CO_2 rise occurs several thousand years prior to melting [4,30,31], so any CO_2 shoaling (i.e., the reversal of CO_2 deepening) and its resulting deep sea CO_3^{2-} spike are predicted to occur early as well, and therefore may be distinguishable from the 'ancillary' effects that come later. Of course, even a uniformly distributed early deglacial shift of CO_2 from the ocean into the atmosphere would have caused a small (<10 μmol kg^{-1}) CO_3^{2-} spike, regardless of mechanism. We prefer the CO_2 shoaling scenario because it is supported by glacial $\delta^{13}C$ data and may be explained by various ventilation, circulation, and biological mechanisms, as outlined above.

What do we know about the preservation history of $CaCO_3$ in the deep ocean? We focus on the Indian and Pacific Oceans since the deep Atlantic is complicated by the waxing and waning of corrosive Southern Ocean waters [12,32,33]. The most basic preservation evidence comes from the abundances of calcareous organisms in sediments, in particular the water depths at which calcite and aragonite begin to decrease significantly (lysoclines) or at which calcite and aragonite fluxes equal their dissolution rates (compensation depths). It has long been recognized that deep Pacific sediments generally contain more $CaCO_3$ during glacial intervals than during interglacials [34]. Over the past 800 ky, the deep Pacific lysocline was ~400 to 800 m deeper during glacials than during interglacials, though several depth maxima appear to fall on deglaciations [35]. The glacial/deglacial CO_3^{2-} increases were estimated to be on the order of 5 μmol kg^{-1}. Berger [36] and Shackleton [24] summarized evidence for a 'global' increase in the compensation depths for pteropods (aragonitic) and foraminifera (calcitic) centered on the last deglaciation. Weight percent $CaCO_3$ also clearly peaks during each of the last six glacial terminations in the very deep (4600 m) southern South Atlantic, a region which may behave like the deep Indo-Pacific [37].

Since the abundance of calcareous organisms in deep sea sediments may also be strongly affected by $CaCO_3$ production rates and dilution by other sedimentary components, it is better to examine more direct proxies of seafloor dissolution. A dissolution index based on planktonic foraminiferal assemblages preserved in sediments suggests a deep Pacific CO_3^{2-} increase of ~5 μmol kg^{-1} at the LGM [38], consistent with the lysocline-based estimate [35]. A composite dissolution index incorporating foraminiferal fragmentation clearly shows that deep Indian Ocean preservation over the past 700 ky was best during deglacial transitions [39]. Foraminiferal fragmentation indices in the eastern equatorial Pacific record a preservation peak during the last deglaciation, though its magnitude appears to be comparable to that of other events within the past glacial–interglacial cycle [40,41]. Broecker et al. [42] used a fragmentation index based on the ratio of coarse fraction $CaCO_3$ to total $CaCO_3$ to identify a Termination I preservation spike in the deep western equatorial Pacific.

Recently, Broecker et al. have generated a series of deep ocean CO_3^{2-} reconstructions based on the weights of planktonic foraminifera. Core top measurements show that the average weight of whole individuals of a given species (within a narrow size range) decreases with decreasing seafloor saturation state [43,44]. This is due to the fact that foraminifera initially thin as they dissolve, before breaking up. Sediment cores from 3.4 and 4.0 km on the Ontong Java Plateau in the western equatorial Pacific display a strong Termination I weight peak, indicative of a preservation maximum [45]. The magnitude of the event appears to decrease with decreasing water

depth, from ~30 μmol kg^{-1} at 4.0 km to no resolvable peak at 2.3 km. A comparable event is seen at 4.4 km in the central equatorial Pacific [46]. There is also evidence for dissolution pulses during MIS 5d, 5b, and the 5/4 transition at 3.4 km on the Ontong Java Plateau, but not shallower [33]. Interpretation of foraminiferal weights is significantly complicated by the observation that initial weights (shell thicknesses) vary with growth environment [44,47]. For example, correcting for greater initial weights under higher surface water CO_3^{2-} [47] shifts LGM deep Pacific CO_3^{2-} reconstructions from slightly higher than modern [45] to ~30–40 μmol kg^{-1} *lower* than modern [48]. This revision is at odds with the previous reconstructions that suggest the glacial deep Pacific was slightly more saturated than today [35,38]. Transient shell weight maxima (minima) are still likely to have been caused by preservation (dissolution) events, but their true magnitudes are currently difficult to estimate.

We conclude that the existing picture of deep Indo-Pacific $CaCO_3$ preservation is broadly consistent with $CaCO_3$ compensation due to CO_2 deepening and shoaling (Fig. 1a) and/or the decay and growth of the terrestrial biosphere, but considerable ambiguity remains.

1.3. Pore water complication

Another important complication for all of these dissolution indices is that significant dissolution occurs as the result of metabolic CO_2 release from decaying organic matter into sediment pore waters [49,50]. It has even been proposed that an ocean-wide change in the ratio of organic to inorganic carbon in sinking biological material could completely decouple the preservation history of $CaCO_3$ from seawater CO_3^{2-} [51]. According to this 'rain ratio' hypothesis, a glacial increase in the ratio of C_{org}:$CaCO_3$ reaching sediments would drive more dissolution within pore waters. As with the CO_2 deepening/$CaCO_3$ compensation hypothesis, the increased dissolution would raise seawater alkalinity, resulting in a rise in CO_3^{2-} and a drop in pCO_2. The steady state of this model is reached when deep water CO_3^{2-} is sufficiently high (more than 50 μmol kg^{-1} higher than today) to balance the excess dissolution being driven by respiratory CO_2 (Fig. 1b). The predicted CO_3^{2-} history is thus sharply different from that of the CO_2 deepening hypothesis, yet the impact on $CaCO_3$ preservation is similar: little net change at steady state, with dissolution (preservation) events across glaciations (deglaciations). Other model results, however, cast doubt on whether higher C_{org}:$CaCO_3$ rain ratios can significantly separate the sedimentary lysocline from the calcite saturation horizon [52]. Support for an extreme version of the rain ratio hypothesis came from benthic foraminiferal boron isotopes ($\delta^{11}B$), which suggested that LGM pH was 0.3 ± 0.1 units higher than today, requiring deep sea CO_3^{2-} to be on the order of 100 μmol kg^{-1} higher [53]. Benthic foraminiferal $\delta^{11}B$ is not as well understood as planktonic however [54], so this interpretation may be questioned.

Even if the rain ratio hypothesis fails to decouple $CaCO_3$ from seawater CO_3^{2-} on a global scale [52], it is clear that localized, transient rain ratio changes have the potential to impact individual or regional dissolution histories. Here we apply a new proxy, benthic foraminiferal Zn/Ca, which appears to directly record past deep ocean CO_3^{2-} rather than dissolution. Hence we can better separate the effects of changing oceanic alkalinity:ΣCO_2 ratios from the effects of pore water processes. Our goal is to evaluate the possible magnitudes of CO_3^{2-} excursions attributable to the CO_2 deepening or rain ratio scenarios, as well as to ancillary carbon cycle changes.

2. Zn/Ca as paleo-CO_3^{2-} proxy

Zn/Ca ratios in shells of the epifaunal benthic foraminifer *Cibicidoides wuellerstorfi* are influenced by dissolved Zn/Ca ratios in the seawater in which they grow [55]. In addition, apparent partition coefficients for Zn, defined as:

$$D_{Zn} = (Zn/Ca)_{foram}/(Zn/Ca)_{seawater} \quad (2)$$

decrease strongly with decreasing seawater calcite saturation state (ΔCO_3^{2-}) (Fig. 2a). A similar influence was shown for D_{Cd} and D_{Ba} by McCorkle et al. [56], who noted that it could represent either reduced incorporation of trace metals in undersaturated waters or post-mortem preferential dissolution. For Zn, at least, the observation of the same effect in Rose Bengal-stained (recently living) individuals argues for an incorporation effect during growth [55]. Also,

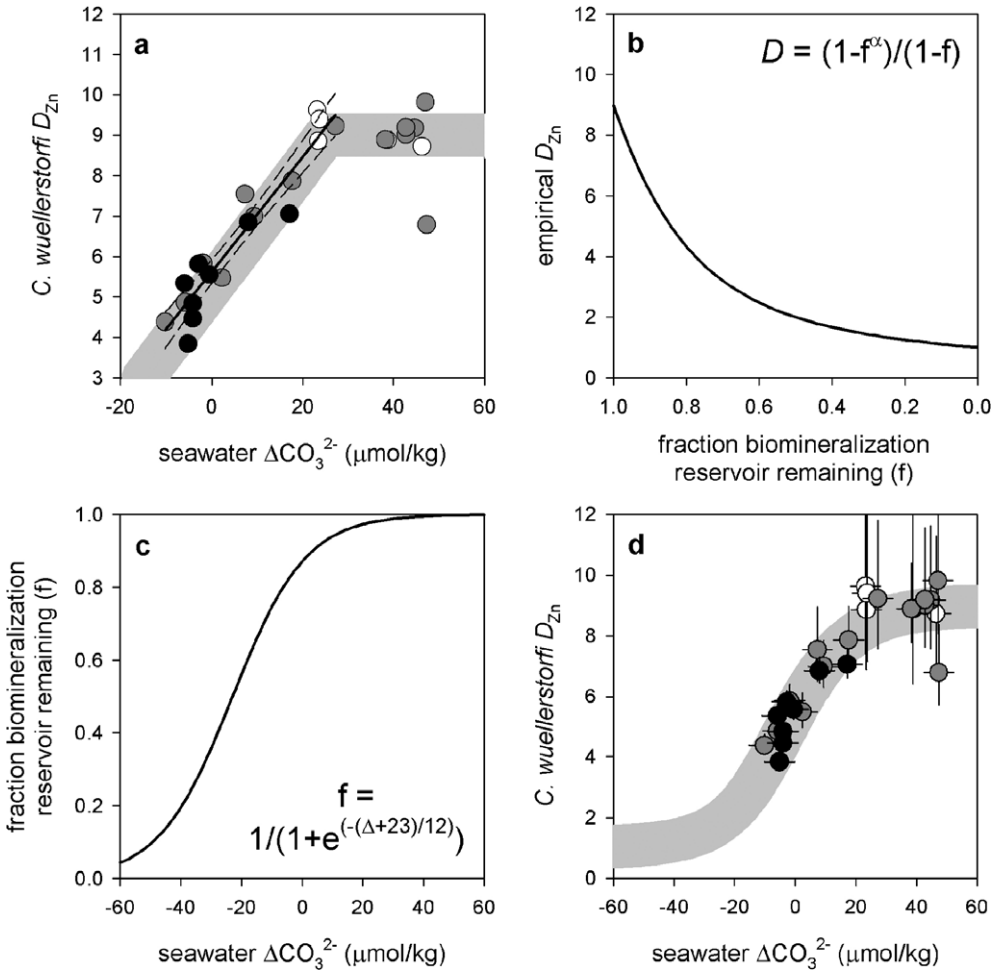

Fig. 2. (a) Zn partition coefficients (D_{Zn}) in *C. wuellerstorfi* vs. seawater ΔCO_3^{2-} [55]. Measurements are from Holocene core tops from the North Atlantic (white), South Atlantic (dark gray), and Indo-Pacific (black). Line shows relationship used here for converting D_{Zn} into ΔCO_3^{2-} (below 30 μmol kg^{-1}) (Eq. (3)), with 95% confidence intervals (dashed). Also shown is the original relationship proposed by Marchitto et al. [55] (gray band). (b–d) Hypothetical biomineralization model that can alternately explain the data in (a) non-linearly. Elderfield et al.'s [64] biomineralization model (b) shows Rayleigh behavior of D_{Zn} as a function of the fraction (f) of an internal reservoir remaining before it is flushed out or replenished with seawater (α=9). When combined with (c), a hypothetical sigmoidal relationship between f and ΔCO_3^{2-} (based on the assumption of less frequent flushing in undersaturated waters), this yields the relationship shown in (d). Constants in (c) were chosen to give a good fit in (d). Panel (d) shows the same data as in (a), but with error bars that approximate the uncertainties in seawater Zn (based on scatter in seawater Zn:Si relationship [55]) and ΔCO_3^{2-} ($\pm$5 μmol kg^{-1}).

laboratory experiments show no decrease in benthic foraminiferal Zn/Ca or Cd/Ca as dissolution proceeds [55,57]. Benthic foraminifera are believed to be more chemically homogenous than planktonic foraminifera, and therefore not subject to the same dissolution artifacts [58]. Hence if some constraints can be placed on past seawater Zn concentrations, Zn/Ca can be used to infer paleo-ΔCO_3^{2-} at the time of growth. We focus here on the deep tropical Pacific, where glacial–interglacial changes in circulation and nutrient content are believed to have been minimal [13,59,60]. Past changes in deep Pacific ΔCO_3^{2-} will have been dominated by varying CO_3^{2-}, since changes in the pressure, salinity, and temperature effects on the saturation CO_3^{2-} value are small and offsetting (about−2, +0.5, and +2 μmol kg^{-1}, respectively, at

the LGM) [61–63]. Although we also present Cd/Ca data below, we consider D_{Cd} to be an imprecise paleo-CO_3^{2-} proxy because of the greater amount of scatter in the D_{Cd}:ΔCO_3^{2-} relationship (Fig. 3).

The ΔCO_3^{2-} effect on D_{Zn} appears to level off above roughly 20–30 μmol kg^{-1}. For simplicity in converting Zn/Ca to paleo-CO_3^{2-}, we assume a linear relationship below ~30 μmol kg^{-1}:

$$D_{Zn} = 0.143\Delta CO_3^{2-} + 5.63 \quad (3)$$

(r^2=0.91, P<0.0001) (Fig. 2a). However, we also demonstrate how a simple calcification model could theoretically explain the relationship non-linearly. Elderfield et al. [64] proposed that trace metal incorporation during benthic foraminiferal calcification occurs via Rayleigh distillation from an internal biomineralization reservoir. If an infinitely small portion of the reservoir is used before it is flushed out or replenished, D will be equal to some preferred fractionation factor α. As more of the reservoir is consumed, D approaches 1 asymptotically (Fig. 2b). We can further hypothesize that in undersaturated waters, the foraminifer must do more work to raise the saturation state of its internal reservoir; hence frequent flushing is disadvantageous and more of the reservoir is used up. A sigmoidal relationship between the fraction of the reservoir remaining and ΔCO_3^{2-} seems reasonable, with values approaching 0 in very undersaturated waters and 1 in very supersaturated waters (Fig 2c). Combined with the Rayleigh distillation equation, this results in a sigmoidal relationship between D and ΔCO_3^{2-} that fits the Zn observations reasonably well (Fig. 2d). This solution is not unique, since several unknown variables can be adjusted. For this reason we stick with the simple linear relationship (Eq. (3)) here.

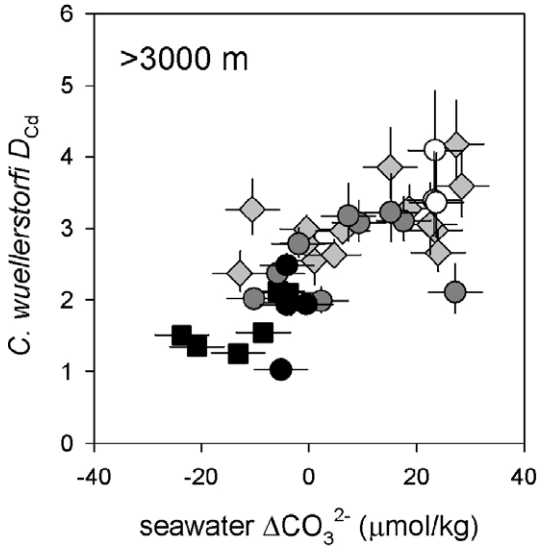

Fig. 3. Relationship between *C. wuellerstorfi* Cd partition coefficients (D_{Cd}) and seawater ΔCO_3^{2-} for core tops below 3000 m water depth (shallower cores are complicated by a significant depth influence on D_{Cd} [60]). Circles are our unpublished data from the North Atlantic (white), South Atlantic (dark gray), and Indo-Pacific (black) (cores given in [55]). Gray diamonds are global data from Boyle [57,60], and black squares are western tropical Pacific data from McCorkle et al. [56] with recalculated ΔCO_3^{2-}. Error bars approximate the uncertainties in seawater Cd (based on scatter in seawater Cd:PO_4 relationship [57]) and ΔCO_3^{2-} (±5 μmol kg^{-1}).

3. Materials and methods

Analyses were made on three deep Pacific cores: RC13-114 (1°39′S, 103°38′W, 3436 m) and ODP 849 (0°11′N, 110°31′W, 3851 m) in the eastern equatorial Pacific, and MW91-9-56BC (0°0′S, 161°47′E, 4041 m) near the Ontong Java Plateau in the western equatorial Pacific. Modern bottom water properties (Table 1) were estimated from nearby WOCE hydrographic stations P18-141 (1°20′S, 110°20′W) and P13-78 (0°1′N, 164°55′E) (http://whpo.ucsd.edu). Dissolved Zn was estimated from dissolved Si [55], dissolved Cd was estimated from dissolved P [57], and ΔCO_3^{2-} was calculated from total alkalinity and ΣCO_2 [65]. Dissolved Ca was taken to be 0.1 mol kg^{-1} [60].

Zn, Cd, and Mn concentrations were measured in shells of the benthic foraminifer *C. wuellerstorfi*. Each sample consisted of ~5–15 individuals (>250 μm) and was reductively and oxidatively cleaned following the methods of Boyle and Keigwin [59] as modified by Boyle and Rosenthal [58]. Samples were generally kept covered when outside of laminar flow benches to minimize the risk of dust-borne contamination, which has historically been a major obstacle to Zn work [66]. Zn, Cd, and Mn were measured sequentially by graphite furnace atomic absorption spectrophotometry (AAS) and Ca was measured by flame AAS, all on a Hitachi Z-8200. Analytical precision, based on frequent analyses of three consistency standards, is

Table 1
Core locations and estimated seawater chemistry

Core	Coordinates	Depth (m)	ΔCO_3^{2-} (μmol/kg)	[Zn] (nmol/kg)	[Cd] (nmol/kg)
RC13-114	1°39′S, 103°38′W	3436	−5	8.8	0.75
ODP 849	0°11′N, 110°31′W	3851	−6	8.6	0.73
MW91-9-56BC	0°0′S, 161°47′E	4041	−13	7.9	0.68

±2–3% for Zn, ±3–6% for Cd, ±8–9% for Mn, and ±1% for Ca (1σ).

Benthic stable isotope samples each consisted of 1–2 *C. wuellerstorfi* (RC13-114 and ODP 849) or 2–3 *Cibicidoides* spp. (MW91-9-56BC) (>250 μm). RC13-114 planktonic stable isotope samples each consisted of 10 *Globigerinoides sacculifer* or 10 *Neogloboquadrina dutertrei* (355–425 μm). Samples were analyzed on a Micromass Optima mass spectrometer with analytical precision of ±0.06‰ for $\delta^{18}O$ and ±0.05‰ for $\delta^{13}C$ (1σ), and on a Finnigan MAT 252 mass spectrometer with analytical precision of ±0.07‰ for $\delta^{18}O$ and ±0.03‰ for $\delta^{13}C$.

Two RC13-114 AMS radiocarbon dates from the planktonic foraminifer *N. dutertrei* (>300 μm) were converted to calibrated ages using the CALIB-98 program with no ΔR reservoir correction [67]. *Pulleniatina obliquiloculata* radiocarbon ages from MW91-9-56BC ([45], W. Broecker, personal communication, 2003) were calibrated in the same way. Average *N. dutertrei* masses (355–425 μm) were measured in RC13-114 following the methods of Broecker and Clark [44]. Planktonic foraminiferal fragmentation was measured in ODP 849 following the methods of Le et al. [40].

Nd isotopes were measured on leachates of fine fraction (<63 μm) bulk sediment in RC13-114, following the methods of Rutberg et al. [68]. $CaCO_3$ was removed by dissolution in buffered acetic acid, and Fe–Mn fractions were leached using hydroxylamine hydrochloride. Rare earth elements were isolated with Eichrom's TRU resin, and Nd separated with α-hydroxyisobutyric acid on AG50-X4 cation resin. Measurement was by dynamic multicollection as NdO^+ on a VG Sector 54 thermal ionization mass spectrometer (TIMS). Measurements of the Nd standard, La Jolla, over the interval of the analyses yielded 0.511849±0.000023 (2σ, n=14). The accepted value for La Jolla is 0.511865, and samples were corrected to this value.

4. Results

4.1. Eastern equatorial Pacific (RC13-114 and ODP 849)

C. wuellerstorfi $\delta^{18}O$ measurements indicate that the top 4 m of RC13-114 span MIS 1 through 6, or roughly the past 150 ky (Fig. 4). Resulting sedimentation rates average ~2–3 cm ky^{-1}. *C. wuellerstorfi* Zn/Ca values range from 2.9 to 7.4 μmol/mol over this interval, with highest values occurring during the last deglaciation, the early Holocene, and interglacial stage 5e. The most prominent feature in the record is the deglacial to early Holocene spike. The predicted modern Zn/Ca value of 4.3 μmol mol^{-1}, based on modern seawater Zn and ΔCO_3^{2-} (Table 1), is in good agreement with the core top value of 4.2 μmol mol^{-1}. If ΔCO_3^{2-} were held constant, the downcore Zn/Ca data would correspond to a seawater Zn range of 5.9–15.1 nmol kg^{-1}. This far exceeds the entire modern deep (27.8 σ_θ) South Pacific to North Pacific Zn gradient of ~6.0–9.6 nmol kg^{-1}, suggesting that the Zn/Ca record is dominated by changes in ΔCO_3^{2-}. RC13-114 Cd/Ca ranges from 0.10 to 0.24 μmol mol^{-1} and follows a similar pattern to Zn/Ca overall. Using a reasonable estimate of ~2 for the predicted modern D_{Cd} (Fig. 3), the predicted Cd/Ca of 0.15 μmol mol^{-1} is close to the core top value of 0.13 μmol mol^{-1}. Holding D_{Cd} constant results in a downcore seawater Cd range of 0.50−1.2 nmol kg^{-1}, again significantly exceeding the modern deep Pacific gradient of ~0.62−0.77 nmol kg^{-1} and pointing to the important role of ΔCO_3^{2-}. Existing deep eastern tropical Pacific Cd/Ca records, based on the genus *Uvigerina*, are comparable [59,60].

Average weights of the planktonic foraminifer *N. dutertrei* (355–425 μm) offer an independent assessment of ΔCO_3^{2-} changes in RC13-114 (Fig. 4). In agreement with the trace metal data and with previous foraminiferal weight results [45,46], there is a

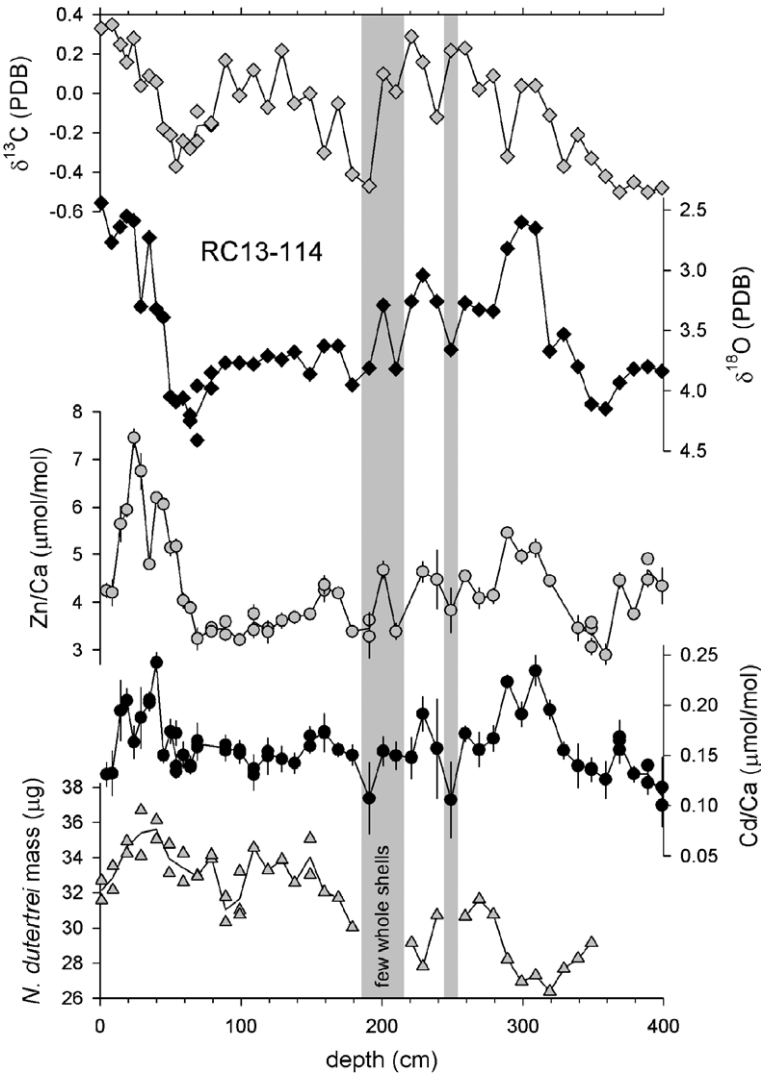

Fig. 4. *C. wuellerstorfi* δ^{13}C (gray diamonds), δ^{18}O (black diamonds), Zn/Ca (gray circles), and Cd/Ca (black circles) in core RC13-114 from the eastern equatorial Pacific (3436 m). Trace metal error bars are analytical ($\pm 1\sigma$) and scale with sample size. Two of three isotope measurements from the shallowest sample (1 cm) have glacial values (not shown), indicating some disturbance at the core top; Zn/Ca and Cd/Ca from this depth are also excluded. See Table 1 in Appendix A for other excluded (contaminated) trace metal measurements. Also shown are average weights of *N. dutertrei* (355–425 μm) (gray triangles). Duplicate measurements were made on separate samplings, usually by different workers. Gray bands indicate intervals where reliable measurements could not be made because too few *N. dutertrei* survived dissolution.

prominent preservation spike centered on the last deglaciation. Interestingly, there is no evidence for a similar weight spike during the penultimate deglaciation, neither in RC13-114 nor in a previously published record from 3.4 km on the Ontong Java Plateau [33]. This apparent discrepancy might result from complicating factors like variable initial shell weights or pore water dissolution, as discussed in Sections 1.2 and 1.3. Notably there are two intervals, during the middle of stage 5 and close to the 5/4 boundary, that contained too few whole *N. dutertrei* for reliable measurements to be made. These severely dissolved intervals, which have been noted previously on the Ontong Java Plateau [33], are also characterized by low trace metal ratios (especially Cd/Ca) suggestive of low ΔCO_3^{2-}.

We analyzed approximately the same time interval (MIS 1–6) in nearby ODP 849, which has a slightly higher sedimentation rate than RC13-114 (~3–4 cm ky^{-1}). The benthic isotope stratigraphy for ODP 849 was established by Mix et al. [69] and supplemented here with nine new measurements (Fig. 5). As in RC13-114, both Zn/Ca and Cd/Ca show prominent deglacial to early Holocene spikes and high values during stage 5e. However, most ODP 849 Zn/Ca values are significantly higher than in RC13-114, whereas the proximity of the two sites predicts that their records should be nearly identical. The Cd/Ca agreement is better, with elevated values in ODP 849 generally limited to stage 5. We believe that the cause of the discrepancy is Mn–Ca-carbonate overgrowths. Boyle [70] showed that Mn/Ca ratios of cleaned foraminifera are elevated in sediments whose pore waters contain reduced

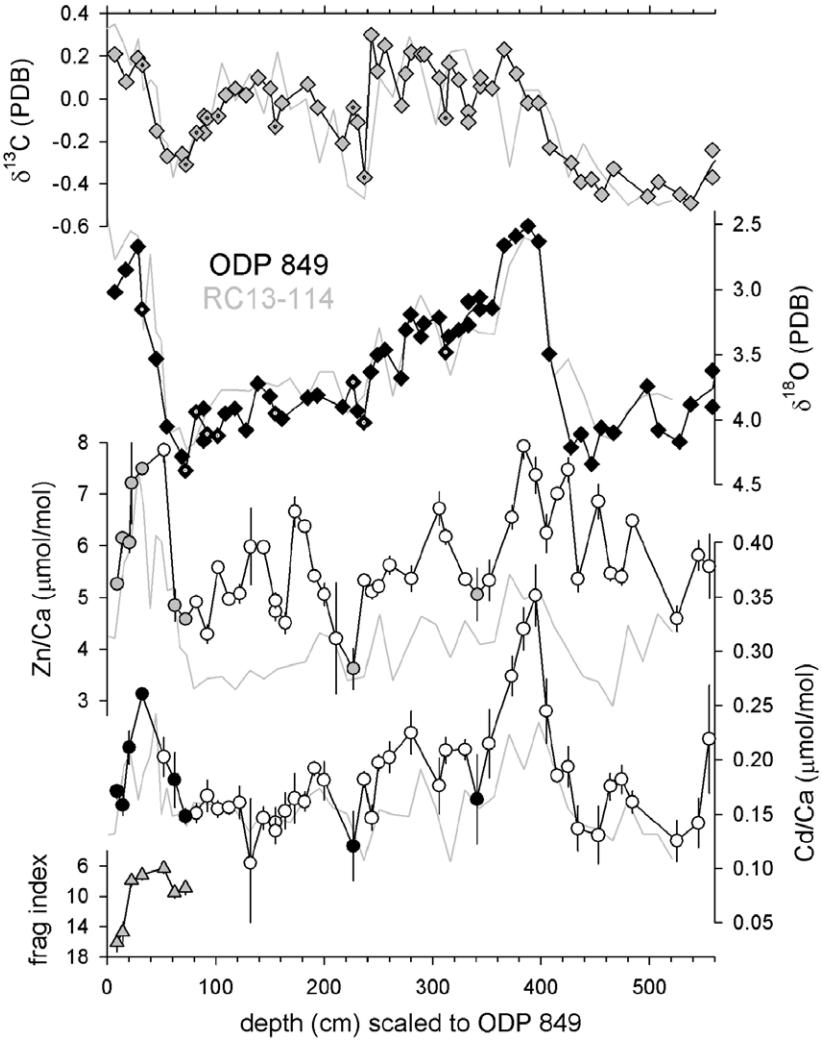

Fig. 5. *C. wuellerstorfi* $\delta^{13}C$ (gray diamonds), $\delta^{18}O$ (black diamonds), Zn/Ca (gray and white circles), and Cd/Ca (black and white circles) in core ODP 849 from the eastern equatorial Pacific (3851 m). Undotted isotope data are from Mix et al. [69]. White trace metal data are from samples with Mn/Ca >200 μmol mol^{-1}, and are therefore considered suspect. Trace metal error bars are analytical ($\pm 1\sigma$) and scale with sample size. Two samples met the size criterion for Zn/Ca (>1 mM Ca) but not for Cd/Ca (>2 mM Ca). Also shown is a foraminiferal fragmentation index (gray triangles, inverted scale) based on the methods of Le et al. [40]. Gray lines show $\delta^{13}C$, $\delta^{18}O$, Zn/Ca, and Cd/Ca in nearby RC13-114, placed on the ODP 849 depth scale using 5 tiepoints based on $\delta^{18}O$.

Mn^{2+}. The Mn appears to be incorporated into a carbonate overgrowth phase that cannot be effectively removed during cleaning because of its similarity to calcite. Cd/Ca data are generally considered suspect when Mn/Ca values exceed ~100–150 μmol mol^{-1} [58]. Mn/Ca in ODP 849 is mostly >200 μmol mol^{-1}, with some samples exceeding 700 μmol mol^{-1} (Fig. 6). Values are particularly high below the visual redox boundary (color change from brown to green) at ~4 m [71]. In contrast, RC13-114 Mn/Ca ratios are all <200 μmol mol^{-1} and mostly <150 μmol mol^{-1}. Thus we conclude that most of the ODP 849 Zn/Ca values (and some of the Cd/Ca values) are contaminated, and limit our paleo-CO_3^{2-} analysis to those samples with Mn/Ca <200 μmol mol^{-1}. Most of the data that characterize the Termination I spike meet this criterion (gray and black circles in Fig. 5).

We also measured a foraminiferal fragmentation index [40] since the LGM in ODP 849 (Fig. 5). This index approximates the percentage of foraminifera that are broken up, assuming that an average foraminifer breaks into ~8 >150 μm pieces. In general agreement with the uncontaminated trace metal data and with the RC13-114 results, fragmentation was reduced during the deglaciation and early Holocene, especially relative to the late Holocene.

4.2. Western equatorial Pacific (MW91-9-56)

MW91-9-56 is the deepest of several Ontong Java Plateau box cores in which Broecker and colleagues identified a Termination I preservation spike [45]. Our *Cibicidoides* spp. $\delta^{18}O$ measurements confirm that this event is centered on the deglaciation (Fig. 7). $\delta^{18}O$ also suggests that the LGM lies at ~30–40 cm, yielding a lower sedimentation rate than either RC13-114 or ODP 849 (~1–2 cm ky^{-1}). *C. wuellerstorfi* Zn/Ca shows only a hint of a deglacial peak. We suspect that three of the four shallowest Zn/Ca measurements are contaminated, thus obscuring the expected decline towards the core top (the predicted modern value is 3.0 μmol mol^{-1}). Note that we encountered frequent laboratory Zn contamination while analyzing RC13-114 (see Table 1 in Appendix A), but were able to replicate measurements there; *C. wuellerstorfi* was too rare in MW91-9-56 to run replicates. Cd/Ca (which is less prone to laboratory contamination) shows a much more obvious decrease since the last deglaciation, suggestive of decreasing ΔCO_3^{2-}. Due to small sample sizes, Mn/Ca was only measured at one depth

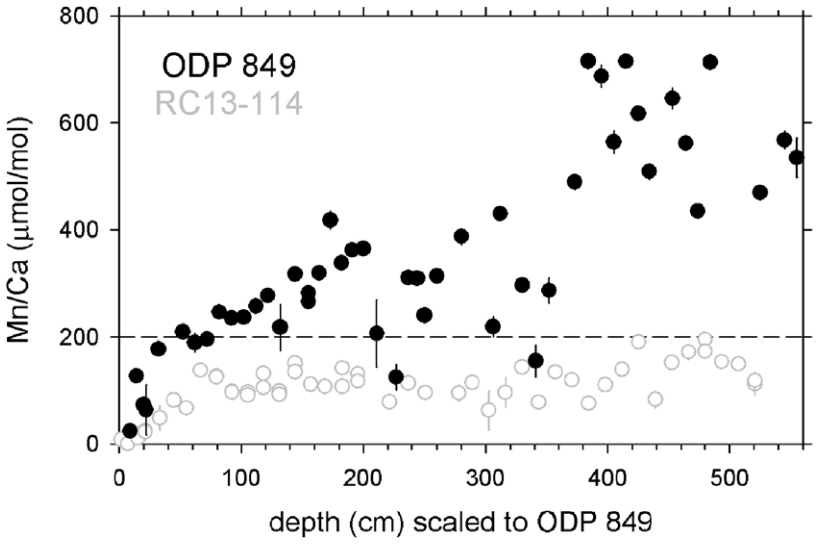

Fig. 6. *C. wuellerstorfi* Mn/Ca in ODP 849 (filled) and RC13-114 (open gray) on the ODP 849 depth scale. Error bars are analytical ($\pm 1\sigma$) and scale with sample size. Dashed line shows the cutoff for samples suspected of authigenic contamination. Visual redox boundary in ODP 849 lies close to 400 cm [71].

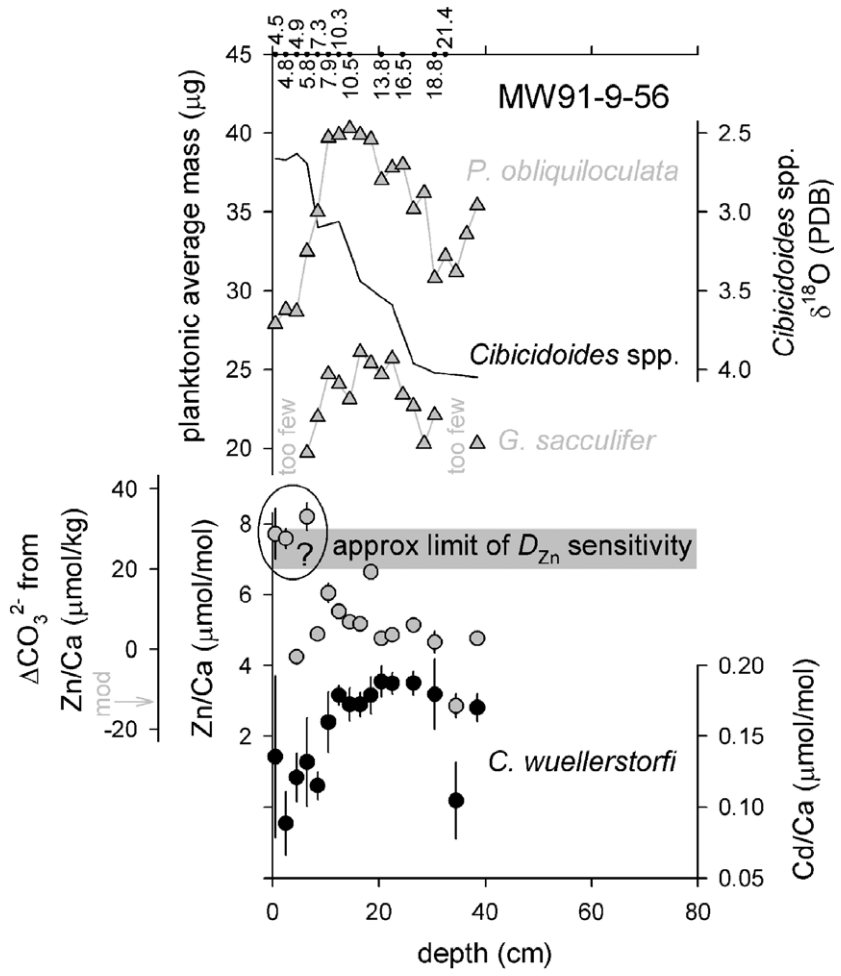

Fig. 7. Bottom: *C. wuellerstorfi* Zn/Ca (gray circles) and Cd/Ca (black circles) in box core MW91-9-56 from the Ontong Java Plateau in the western equatorial Pacific (4041 m). For Zn/Ca, offset axis shows inferred ΔCO_3^{2-} derived by holding seawater Zn at the modern concentration. Arrow indicates modern ΔCO_3^{2-}, and gray band spans ΔCO_3^{2-} values above which D_{Zn} is constant (~20–30 μmol kg^{-1}) (see Fig. 2). Zn/Ca data within oval are suspected of being contaminated. Top: average planktonic foraminiferal weights (gray triangles) in the same core, with heavily dissolved intervals that contained few whole *G. sacculifer* noted [45]. Numbers at top indicate calibrated radiocarbon ages (ky BP) from *P. obiquiloculata* ([45], W. Broecker, personal communication, 2003). *Cibicidoides* spp. $\delta^{18}O$ (black line) is also shown.

(34.5 cm), where it was below our detection limit of 3 μmol/mol.

5. Discussion

5.1. ΔCO_3^{2-} and $CaCO_3$ compensation

As discussed above, Zn/Ca may be converted into D_{Zn}, and thus ΔCO_3^{2-}, if seawater Zn can be independently constrained. The simplest approach for the deep Pacific is to assume that seawater Zn has been constant through time. This is a reasonable first-order assumption because glacial–interglacial changes in circulation and nutrient content are believed to have been minimal in this basin [13,59,60]. As a check on this assumption, we have also measured ε_{Nd} in RC13-114 dispersed Fe–Mn oxides across Termination I. Fe–Mn oxides precipitate as coatings on other phases and as particles, and they record the Nd isotopic composition (ε_{Nd}) of the waters from which they grow [68]. Since different deep water

masses have characteristic ε_{Nd} signatures [72], Fe–Mn phases can be used to reconstruct deep ocean circulation [68,73]. ε_{Nd} is influenced by weathering and volcanic sources but not by biogeochemical cycling, so it offers an assessment independent of the nutrient tracers $\delta^{13}C$, Cd, and Zn. Our results (Fig. 8) suggest that the ε_{Nd} signature of the deep eastern tropical Pacific has varied little since the LGM. If anything, these waters may have become slightly more South Pacific-like (more negative ε_{Nd}) across the deglaciation. If caused by a deep circulation change, we might expect seawater Zn to have decreased slightly, suggesting that seawater Zn did not contribute to the Termination I Zn/Ca spike. Alternatively, we cannot rule out a terrigenous weathering influence on the deep Pacific ε_{Nd} record. Nevertheless, we find no evidence for major changes in deep Pacific circulation since the LGM, in agreement with other proxies [13,59,60].

Inferred RC13-114 ΔCO_3^{2-} values, derived by holding seawater Zn at the modern concentration, range from −16 to 20 μmol kg^{-1} (Fig. 8). The core top value is indistinguishable from the modern estimate of −5 μmol kg^{-1}. The Termination I peak reaches ~25 μmol kg^{-1} higher than modern and ~32 μmol kg^{-1} higher than MIS 2/3 values (note that the

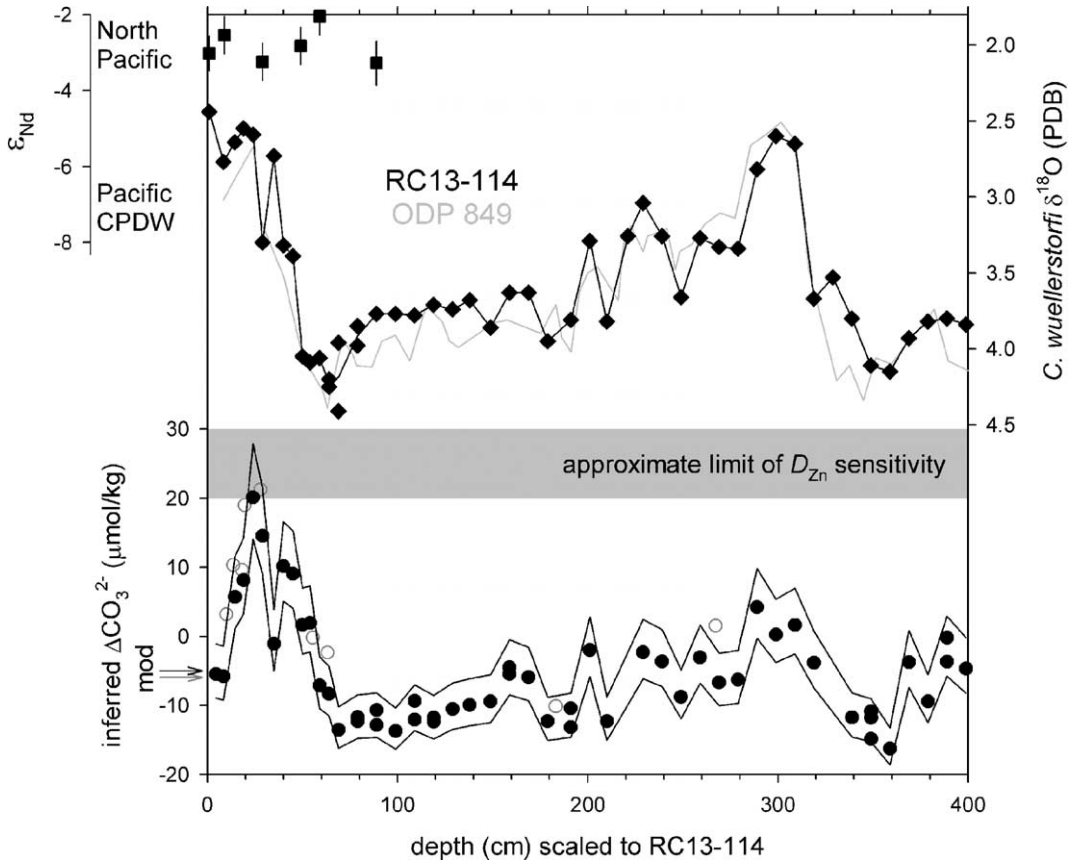

Fig. 8. Bottom: ΔCO_3^{2-} from *C. wuellerstorfi* Zn/Ca in RC13-114 (black circles) and ODP 849 (open gray circles, samples with Mn/Ca <200 μmol mol^{-1} only), derived by holding seawater Zn constant, on RC13-114 depth scale. Envelope around RC13-114 data shows result of increasing or decreasing seawater Zn by 1 nmol kg^{-1} (11%). Arrows show modern ΔCO_3^{2-} at each core site, and gray band spans ΔCO_3^{2-} values above which D_{Zn} is constant (see Fig. 2). Middle: *C. wuellerstorfi* $\delta^{18}O$ in RC13-114 (diamonds) and ODP 849 (gray line). Top: bulk fine fraction ε_{Nd} (black squares) across Termination I in RC13-114. Error bars ($\pm 2\sigma$) account for both in-run error and external error on the standard. Approximate modern seawater ε_{Nd} values for the deep North Pacific and for South Pacific Circumpolar Deep Water (CPDW) are noted. The entire modern deep ocean range in ε_{Nd} is about −3 (North Pacific) to −14 (North Atlantic) [68,72].

peak ΔCO_3^{2-} value could be a minimum estimate because D_{Zn} is approaching the limit of its sensitivity to saturation state). The Termination II peak appears to be smaller in magnitude (<10 μmol kg^{-1} higher than modern), but this may be an issue of sample resolution. The lowest saturation states were reached during glacial stages 2, 4, and 6. Results from uncontaminated (Mn/Ca <200 μmol/mol) ODP 849 samples are in good agreement with the RC13-114 record (open gray circles in Fig. 8). Also, the Termination I peak in western Pacific core MW91-9-56 (such as it is) appears to be of comparable magnitude (Fig. 7). All Termination I estimates compare favorably to the 30 μmol kg^{-1} foraminiferal weight estimate from MW91-9-56 [45].

Overall, the deep Pacific ΔCO_3^{2-} record bears reasonable resemblance to that predicted by the CO_2 deepening/$CaCO_3$ compensation theory (Fig. 1a): slight lows are observed during glacial inceptions, when CO_2 is added incrementally from the upper ocean; and major highs occur on glacial terminations, when CO_2 is returned wholesale to the upper ocean. The relative similarity of modern and steady state glacial ΔCO_3^{2-} values implies that either the global oceanic formation rate of $CaCO_3$ did not change substantially, or that any large change was roughly balanced by a change in the riverine input of alkalinity (see Section 5.3 for discussion of the possible small change in glacial ΔCO_3^{2-}). There is no evidence for the dramatically increased glacial CO_3^{2-} predicted by the rain ratio hypothesis [51] (Fig. 1b).

The Termination I CO_3^{2-} rise appears to precede ice volume (benthic $\delta^{18}O$) by several thousand years, as expected from the early atmospheric CO_2 rise (Fig. 9). Although we are reluctant to over-interpret the single Zn/Ca measurement at 35 cm, the data are suggestive of a double peak across the deglaciation. If this is a robust feature, we suggest that the earlier peak is the result of CO_2 rearrangement within the ocean [6,9] while the latter peak is due to boreal forest regrowth [24,42]. The bulk of forest regrowth must occur late in the deglaciation, after ice sheets have retreated. The radiocarbon age on our second peak (8.3 ky cal BP) is consistent with this scenario.

The model-predicted magnitude of each peak depends not only on how much CO_2 was removed from the deep ocean, but over what time scale. If the CO_2 is removed rapidly, the CO_3^{2-} peak will be maximized; if removed more slowly (over several millennia), the compensation response may begin to reverse the CO_3^{2-} rise before it is completed, resulting in a somewhat broader, smaller-magnitude peak. Various estimates of the early deglacial vertical rearrangement of CO_2 result in maximum (rapid) CO_3^{2-} peaks ranging from ~10 or 15 μmol kg^{-1} [74] to ~30 μmol kg^{-1} ([6,9], R. Toggweiler, personal communication, 2003). Our observation of a roughly 25 μmol kg^{-1} rise spread over several millennia is supportive of the larger estimate. A later terrestrial carbon removal of ~500 Gt (see Section 5.2 for

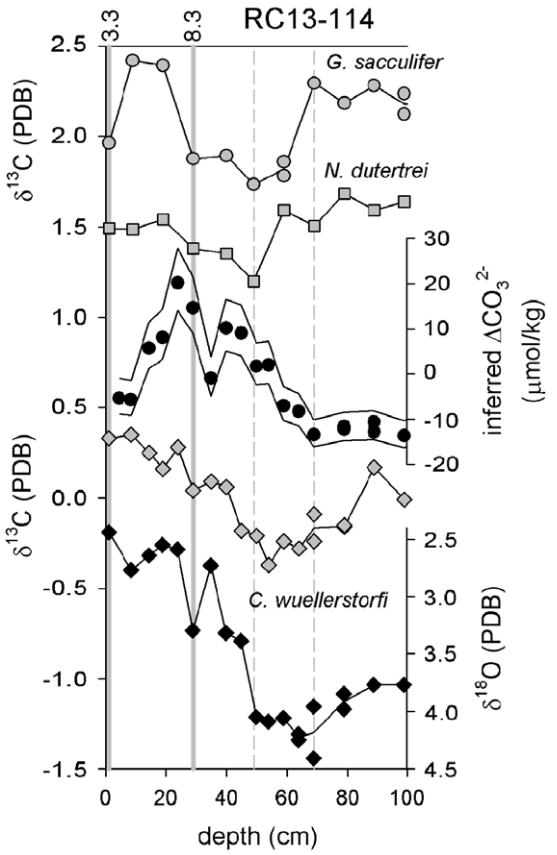

Fig. 9. RC13-114 planktonic foraminiferal $\delta^{13}C$ in the surface-dwelling *G. sacculifer* (gray circles) and the thermocline-dwelling *N. dutertrei* (gray squares). *C. wuellerstorfi* $\delta^{13}C$ (gray diamonds), $\delta^{18}O$ (black diamonds), and Zn/Ca-inferred ΔCO_3^{2-}(black circles) are also shown. Planktonic $\delta^{13}C$ decreases during the interval bounded by the dashed gray lines, coincident with the ΔCO_3^{2-} rise and preceding the benthic $\delta^{13}C$ and $\delta^{18}O$ rises. Gray bands and numbers at top indicate calibrated radiocarbon ages (ky BP) from *N. dutertrei*.

uncertainties), if rapid, would induce a maximum CO_3^{2-} rise on the order of 20 μmol kg^{-1}. Our second peak is also broadly consistent with this estimate. Of course, one must keep in mind that bioturbation is likely to have attenuated the peaks to some degree [75].

We calculate that an early deglacial CO_3^{2-} rise of ~25–30 μmol kg^{-1} requires a CO_2 removal on the order of 50–60 μmol kg^{-1}. Box modeling [9] suggests that a return of 60 μmol kg^{-1} of CO_2 to the surface ocean could have raised atmospheric CO_2 by ~20 ppmv. The ensuing $CaCO_3$ compensation would have then lowered ocean pH and raised atmospheric CO_2 by perhaps an additional 35 ppmv [9]. Together, these two effects can account for more than half of the 90 ppmv atmospheric CO_2 rise since the LGM. This analysis treats the deep tropical Pacific as representative of the global ocean, but it is possible that CO_2 changes and compensation were larger in other basins. $\delta^{13}C$ suggests that CO_2 was particularly elevated in the glacial deep Southern Ocean [76], and percent $CaCO_3$ there seems to follow a strong compensation type pattern [37].

Ridgwell et al. [77] recently proposed an alternative explanation for an early deglacial CO_3^{2-} peak. Rather than terrestrial carbon sequestration lagging behind ice sheet melting, they rely on model results that call for major terrestrial CO_2 fertilization to accompany the atmospheric CO_2 rise [78]. This early removal of CO_2 from the atmosphere–ocean system causes an early rise in deep sea CO_3^{2-}. $CaCO_3$ compensation is only partially able to reverse the CO_3^{2-} rise because the model calls for terrestrial biomass to continue increasing throughout the Holocene. CO_3^{2-} does drop during the late Holocene due to coral reef regrowth during the mid to late Holocene, and compensation has no chance to reverse this effect because of the late timing. The net result of these two processes, separated in time and with little compensation, is a small-magnitude (~10–15 μmol kg^{-1}) Termination I CO_3^{2-} peak. Although we cannot rule out an early increase in terrestrial carbon storage (the main data addressing this issue, oceanic and atmospheric $\delta^{13}C$, are quite complex), we suggest that it would be insufficient to explain most of our observed deep Pacific deglacial CO_3^{2-} rise. If coral reef regrowth models [79] are reasonably accurate, it is likely that corals contributed, by perhaps 10 μmol kg^{-1}, to the observed late Holocene CO_3^{2-} drop. There also remains the possibility that organic matter burial on newly submerged continental shelves [27], if in excess of associated $CaCO_3$ burial, could have offset the coral effect to some degree. Finally, if terrestrial biomass actually *decreased* during the mid to late Holocene [80], the carbon addition to the ocean could have also contributed (by <10 μmol kg^{-1}) to the late Holocene CO_3^{2-} drop [42,45].

5.2. Oceanic $\delta^{13}C$

The early deglacial removal of light metabolic CO_2 from the deep ocean, whether removed to the upper ocean or to land, should have had a positive impact on deep sea $\delta^{13}C$. A deep ocean CO_2 loss of ~50–60 μmol kg^{-1} is expected to raise $\delta^{13}C$ by ~0.5–0.6‰. The mean whole-ocean increase in $\delta^{13}C$ since the last glacial maximum is estimated at ~0.3‰, though data coverage, especially in the upper Pacific, is quite poor [13,60]. This increase is commonly attributed to a deglacial expansion of the terrestrial biosphere by perhaps 400–500 Gt of carbon, assuming that the mean isotopic composition of the terrestrial carbon is known [24–26]. The terrestrial biosphere estimate ignores any changes in storage of organic carbon on continental shelves [25] and the possible influence of methane release from permafrost and/or ocean margin clathrates [81]. Independent reconstructions based on paleoecological data tend to argue for a larger Holocene expansion of the terrestrial biosphere, by up to 2 or 3 times that inferred from the marine data [82,83]. It may be concluded that the terrestrial biosphere impact on deep sea $\delta^{13}C$ across Termination I is poorly constrained.

The LGM to Holocene $\delta^{13}C$ shift is roughly 0.4–0.6‰ in the deep tropical Pacific, or ~0.1–0.3‰ in excess of the whole-ocean estimate (e.g., [20,60,69,84]) (Figs. 4 and 5). In contrast to the early timing of the deglacial CO_3^{2-} rise, however, the $\delta^{13}C$ increase is in phase with (or perhaps even lags) $\delta^{18}O$ (Fig. 9). We therefore require the expected early $\delta^{13}C$ rise to be 'masked' by some concurrent process. One promising candidate is clathrate methane addition to the global atmosphere–ocean system. Methane stored in permafrost and ocean margin clathrates is isotopically very light, ranging from ~−40‰ to −100‰ [81]. If a significant portion of the

early deglacial atmospheric methane rise came from these sources, there would be a considerable impact on oceanic $\delta^{13}C$ (tropical wetland and temperate wetland-peatland methanogenesis, in contrast, has little isotopic impact). Intermediate water warming could theoretically destabilize clathrates in advance of ice sheet melting [85]. Maslin and Thomas [81] recently suggested that a deglacial release of only 1% of the global clathrate reservoir, accounting for <30% of the total atmospheric methane rise, would have reduced oceanic $\delta^{13}C$ by ~0.2‰.

We also expect to see isotopic evidence of early deglacial CO_2 shoaling in the upper ocean. Shackleton et al.'s [23] planktonic-benthic $\delta^{13}C$ difference clearly decreased ahead of ice volume, not because of an early benthic rise but because of an early planktonic drop (note, however, that their benthic record is based on *Uvigerina*, which is not as reliable as *Cibicidoides*). The early planktonic $\delta^{13}C$ drop is part of a Termination I minimum commonly seen in the Indo-Pacific and South Atlantic [86]. Spero and Lea [86] attribute the planktonic $\delta^{13}C$ minimum to the upwelling of CO_2 previously trapped in the deep ocean. They suggest that the CO_2 was returned to the surface via renewed Circumpolar Deep Water upwelling in the Southern Ocean and transmitted to other basins (including the eastern tropical Pacific) by Antarctic Intermediate Water. The deglacial planktonic $\delta^{13}C$ drop may be synchronous with Antarctic warming, spanning ~20 to 16 ky cal BP. In RC13-114, the $\delta^{13}C$ decrease is seen in both *G. sacculifer* (mixed layer dweller) and *N. dutertrei* (lower thermocline dweller) (Fig. 9). Although the two species are not perfectly synchronized, both clearly lead the benthic $\delta^{13}C$ and are coincident with the early deglacial Zn/Ca rise.

In summary, we suggest that the early planktonic $\delta^{13}C$ drop represents the return of CO_2 to the upper (surface) ocean, with the deep Pacific $\delta^{13}C$ response (rise) being masked by another mechanism. The subsequent increase in deep Pacific $\delta^{13}C$ (by ~0.4–0.6‰) may include the latter part of CO_2 shoaling, followed by the bulk of terrestrial biosphere regrowth.

5.3. Seawater Zn and Cd

The above discussion assumes constant deep tropical Pacific Zn concentrations through time. Aside from changes in deep circulation (believed to have been small), deep water Zn, and Cd, may potentially vary with changes in the elements' oceanic inventories. The oceanic residence time for Zn is probably on the order of 10–30 ky, given rough estimates of riverine [87], aeolian [88], and high-temperature hydrothermal [89] inputs. The residence time for Cd has been estimated at ~25 ky, assuming that hydrothermal sources are minor [90]. Thus inventory changes on glacial–interglacial timescales are within the realm of possibility for both elements, with the largest differences most likely occurring at the LGM. No estimate exists for the LGM inventory of Zn, but Cd has been calculated to have been within ~13% of its modern abundance [60]. The envelope in Fig. 8 shows the impact of increasing or decreasing seawater Zn by 1 nmol kg^{-1}, or 11%. If Zn truly remained within these bounds, then glacial ΔCO_3^{2-} appears to have been slightly lower than today, in contrast to lysocline inferences of slightly higher than today [35,38]. A slight deepening of the glacial lysocline in spite of lower ΔCO_3^{2-} might point to increased $CaCO_3$ rain rates, with the increased deep sea burial possibly balancing reduced burial on continental shelves and/or increased alkalinity input via rivers. Confirmation of glacial ΔCO_3^{2-} levels will require an eventual evaluation of the glacial Zn inventory, based on globally distributed Zn/Ca data.

Another mechanism that could potentially cause deep Pacific Zn and Cd to vary is the same mechanism that vertically transferred the CO_2. Toggweiler [9] noted that his Southern Ocean ventilation mechanism is able to move CO_2 independently of nutrients because CO_2 is a gas. Thus his glacial deep ocean accumulates CO_2 without accumulating Zn or Cd. If CO_2 deepening occurred by some other mechanism that was not able to decouple CO_2 from nutrients, Zn is much less likely than Cd to have been affected. This is because Zn behaves like a refractory nutrient (is depleted in the upper ocean) while Cd, like organic carbon, behaves like a labile nutrient (has an intermediate-depth maximum). A coupling between Cd and CO_2 could explain why the deglacial Cd/Ca peak in RC13-114 seems to lag the Zn/Ca peak. That is, deep water Cd may have been decreasing at the same time that CO_3^{2-} was increasing, leading to offsetting effects on Cd/Ca. Alternatively, the uncertain relationship between D_{Cd} and ΔCO_3^{2-} might explain the discrepancy.

6. Conclusions

The ΔCO_3^{2-} history of the deep tropical Pacific over the last glacial–interglacial cycle is broadly consistent with the predictions of the CO_2 deepening/$CaCO_3$ compensation hypothesis. Slight CO_3^{2-} lows occur during the progression towards maximum glaciation, as CO_2 is incrementally added to the deep ocean; and a major CO_3^{2-} peak occurs during deglaciation, as CO_2 is returned to the upper ocean. The inferred magnitude of the Termination I peak, ~25–30 μmol kg^{-1}, suggests that $CaCO_3$ compensation alone may explain more than one third of the 90 ppmv glacial lowering of atmospheric CO_2 [9]. An apparent secondary peak during the early Holocene may represent the regrowth of boreal forests.

This study represents only a first attempt at using Zn/Ca to infer deep ocean paleo-CO_3^{2-}. Our conclusions regarding $CaCO_3$ compensation require verification at other deep Indo-Pacific sites. In particular, the magnitude of CO_3^{2-} changes may be depth-dependent, as suggested by foraminiferal weight results [45]. Increased spatiotemporal coverage should also place constraints on possible variations in the oceanic Zn inventory, allowing us to better isolate the effects of ΔCO_3^{2-}. Finally, continued application of multiple paleo-CO_3^{2-} proxies is crucial for improving our understanding of the global carbon cycle.

Acknowledgements

We thank A. Koutavas for providing unpublished *G. sacculifer* $\delta^{13}C$ data; L. Baker, J. Bauer, G. Fails, P. Malone, and D. Ostermann for assistance with core sampling, foram picking, and stable isotope analyses; N. G. Hemming for assistance with ε_{Nd} analyses; W. Broecker for access to washed MW91-9-56 material; and W. Curry, D. Oppo, and A. van Geen for use of their lab facilities. D. Anderson, D. Sigman, J.R. Toggweiler, and an anonymous reviewer provided valuable comments that improved this manuscript. RC13-114 is curated at LDEO with support from the NSF and ONR. MW91-9-56 is curated at WHOI with support from the NSF, ONR, and USGS. This work was supported by a JOI/USSAC Ocean Drilling Fellowship (JSG-CY 124), WHOI's R.H. Cole Ocean Ventures Fund, the LDEO Postdoctoral Fellowship Program, LynchStieglitz's NSF CAREER award (OCE9984989), and Marchitto's startup funds at INSTAAR.

Appendix A. Supplementary data

Supplementary data associated with this article can be found, in the online version, at doi:10.1016/j.epsl.2004.12.024.

References

[1] J.-R. Petit, J. Jouzel, D. Raynaud, N.I. Barkov, J.-M. Barnola, I. Basile, M. Bender, J. Chappellaz, M. Davis, G. Delaygue, M. Delmotte, V.M. Kotlyakov, M. Legrand, V.Y. Lipenkov, C. Lorius, L. Pepin, C. Ritz, E. Saltzman, M. Stievenard, Climate and atmospheric history of the past 420,000 years from the Vostok ice core, Antarctica, Nature 399 (1999) 429–436.

[2] A. Neftel, E. Moor, H. Oeschger, B. Stauffer, Evidence from polar ice cores for the increase in atmospheric CO_2 in the past two centuries, Nature 315 (1985) 45–47.

[3] C.D. Keeling, T.P. Whorf, Atmospheric CO_2 records from sites in the SIO air sampling network, Trends: A Compendium of Data on Global Change, Carbon Dioxide Information Analysis Center, Oak Ridge National Laboratory, U.S. Department of Energy, Oak Ridge, TN, 2003.

[4] W.S. Broecker, G.M. Henderson, The sequence of events surrounding Termination II and their implications for the cause of glacial-to-interglacial CO_2 changes, Paleoceanography 13 (1998) 352–364.

[5] W.S. Broecker, T.-H. Peng, The role of $CaCO_3$ compensation in the glacial to interglacial atmospheric CO_2 change, Glob. Biogeochem. Cycles 1 (1987) 15–29.

[6] E.A. Boyle, The role of vertical chemical fractionation in controlling Late Quaternary atmospheric carbon dioxide, J. Geophys. Res. 93 (1988) 15701–15714.

[7] R.S. Keir, On the late Pleistocene ocean geochemistry and circulation, Paleoceanography 3 (1988) 413–445.

[8] R. Francois, M.A. Altabet, E.-F. Yu, D.M. Sigman, M.P. Bacon, M. Frank, G. Bohrmann, G. Bareille, L.D. Labeyrie, Contribution of Southern Ocean surface-water stratification to low atmospheric CO_2 concentrations during the last glacial period, Nature 389 (1997) 929–935.

[9] J.R. Toggweiler, Variation of atmospheric CO_2 by ventilation of the ocean's deepest water, Paleoceanography 14 (1999) 571–588.

[10] D.M. Sigman, E.A. Boyle, Glacial/interglacial variations in atmospheric carbon dioxide, Nature 407 (2000) 859–869.

[11] B.B. Stephens, R.F. Keeling, The influence of Antarctic sea ice on glacial–interglacial CO_2 variations, Nature 404 (2000) 171–174.

[12] E.A. Boyle, L.D. Keigwin, North Atlantic thermohaline circulation during the past 20,000 years linked to high-latitude surface temperature, Nature 330 (1987) 35–40.
[13] J.C. Duplessy, N.J. Shackleton, R.G. Fairbanks, L. Labeyrie, D. Oppo, N. Kallel, Deepwater source variations during the last climatic cycle and their impact on global deepwater circulation, Paleoceanography 3 (1988) 343–360.
[14] D.W. Oppo, S.J. Lehman, Mid-depth circulation of the subpolar North Atlantic during the last glacial maximum, Science 259 (1993) 1148–1152.
[15] J.H. Martin, S.E. Fitzwater, Iron deficiency limits phytoplankton growth in the north–east Pacific subarctic, Nature 331 (1988) 341–343.
[16] N. Kumar, R.F. Anderson, R.A. Mortlock, P. Froelich, P. Kubick, B. Dittrick-Hannen, M. Suter, Increased biological productivity and export production in the glacial Southern Ocean, Nature 378 (1995) 675–680.
[17] P.G. Falkowski, Evolution of the nitrogen cycle and its influence on the biological sequestration of CO_2 in the ocean, Nature 387 (1997) 272–275.
[18] N.C. Slowey, W.B. Curry, Glacial–interglacial differences in circulation and carbon cycling within the upper western North Atlantic, Paleoceanography 10 (1995) 715–732.
[19] N. Kallel, L.D. Labeyrie, A. Juillet-Leclerc, J.-C. Duplessy, A deep hydrological front between intermediate and deep-water masses in the glacial Indian Ocean, Nature 333 (1988) 651–655.
[20] J.C. Herguera, E. Jansen, W.H. Berger, Evidence for a Bathyal front at 2000-M depth in the glacial Pacific, Based on a depth transect on Ontong Java Plateau, Paleoceanography 7 (1992) 273–288.
[21] L.D. Keigwin, Glacial-age hydrography of the far northwest Pacific Ocean, Paleoceanography 13 (1998) 323–339.
[22] K. Matsumoto, T. Oba, J. Lynch-Stieglitz, H. Yamamoto, Interior hydrography and circulation of the glacial Pacific Ocean, Quat. Sci. Rev. 21 (2002) 1693–1704.
[23] N.J. Shackleton, M.A. Hall, J. Line, C. Shuxi, Carbon isotope data in core V19-30 confirm reduced carbon dioxide concentration in the ice age atmosphere, Nature 306 (1983) 319–322.
[24] N.J. Shackleton, Carbon-13 in Uvigerina: tropical rainforest history and the Equatorial Pacific carbonate dissolution cycles, in: N.R. Andersen, A. Malahoff (Eds.), $_2$ In The Oceans, Plenum, New York, 1977, pp. 401–427.
[25] T.J. Crowley, Ice age carbon, Nature 352 (1991) 575–576.
[26] M.I. Bird, J. Lloyd, G.D. Farquhar, Terrestrial carbon storage at the LGM, Nature 371 (1994) 566.
[27] W.S. Broecker, Glacial to interglacial changes in ocean chemistry, Prog. Oceanogr. 11 (1982) 151–197.
[28] R.S. Keir, W.H. Berger, Late Holocene carbonate dissolution in the equatorial Pacific: reef growth or Neoglaciation? in: E.T. Sundquist, W.S. Broecker (Eds.), The Carbon Cycle and Atmospheric CO_2: Natural Variations Archean to Present, vol. 32, American Geophysical Union, Washington, DC, 1985, pp. 208–219.
[29] J.C.G. Walker, B.C. Opdyke, Influence of variable rates of neritic carbonate deposition on atmospheric carbon dioxide and pelagic sediments, Paleoceanography 10 (1995) 415–427.
[30] T. Sowers, M. Bender, Climate records covering the last deglaciation, Science 269 (1995) 210–214.
[31] N.J. Shackleton, The 100,000-year ice-age cycle identified and found to lag temperature, carbon dioxide, and orbital eccentricity, Science 289 (2000) 1897–1902.
[32] T.M. Marchitto, D.W. Oppo, W.B. Curry, Paired benthic foraminiferal Cd/Ca and Zn/Ca evidence for a greatly increased presence of Southern Ocean Water in the glacial North Atlantic, Paleoceanography 17 (2002) 1038.
[33] W.S. Broecker, E. Clark, $CaCO_3$ dissolution in the deep sea: paced by insolation cycles, Geochem. Geophys. Geosystems 4 (2003) 1059.
[34] G.O.S. Arrhenius, Sediment cores from the east Pacific, Rep. Swed. Deep Sea Exped. 1947–48 5 (1952) 1–228.
[35] J.W. Farrell, W.L. Prell, Climatic change and $CaCO_3$ preservation: an 800,000 year bathymetric reconstruction from the central equatorial Pacific Ocean, Paleoceanography 4 (1989) 447–466.
[36] W.H. Berger, Deep-sea carbonate and the deglaciation preservation spike in pteropods and foraminifera, Nature 269 (1977) 301–304.
[37] D.A. Hodell, C.D. Charles, F.J. Sierro, Late Pleistocene evolution of the ocean's carbonate system, Earth Planet. Sci. Lett. 192 (2001) 109–124.
[38] D.M. Anderson, D. Archer, Glacial–interglacial stability of ocean pH inferred from foraminifer dissolution rates, Nature 416 (2002) 70–73.
[39] L.C. Peterson, W.L. Prell, Carbonate preservation and rates of climatic change: an 800 kyr record from the Indian Ocean, in: E.T. Sundquist, W.S. Broecker (Eds.), The carbon cycle and atmospheric CO_2: natural variations Archean to present, Geophysical Monograph, vol. 32, American Geophysical Union, Washington, DC, 1985, pp. 251–269.
[40] J. Le, A.C. Mix, N.J. Shackleton, Late Quaternary paleoceanography in the eastern equatorial Pacific Ocean from planktonic foraminifers: a high-resolution record from Site 846, in: N.G. Pisias, L.A. Mayer, T.R. Janecek, A. Palmer-Julson, T.H. van Andel (Eds.), Proceedings of the Ocean Drilling Program, Scientific Results, vol. 138, Ocean Drilling Program, College Station, TX, 1995, pp. 675–693.
[41] V.S. McKenna, J.W. Farrell, D.W. Murray, S.C. Clemens, The foraminifer record at Site 847: paleoceanographic response to Late Pleistocene climate variability, in: N.G. Pisias, L.A. Mayer, T.R. Janecek, A. Palmer-Julson, T.H. van Andel (Eds.), Proceedings of the Ocean Drilling Program, Scientific Results, vol. 138, Ocean Drilling Program, College Station, TX, 1985, pp. 695–716.
[42] W.S. Broecker, E. Clark, D.C. McCorkle, T.-H. Peng, I. Hajdas, G. Bonani, Evidence for a reduction in the carbonate ion content of the deep sea during the course of the Holocene, Paleoceanography 14 (1999) 744–752.
[43] G.P. Lohmann, A model for variation in the chemistry of planktonic foraminifera due to secondary calcification and selective dissolution, Paleoceanography 10 (1995) 445–457.

[44] W.S. Broecker, E. Clark, An evaluation of Lohmann's foraminifera weight dissolution index, Paleoceanography 16 (2001) 531–534.
[45] W.S. Broecker, J. Lynch-Stieglitz, E. Clark, I. Hajdas, G. Bonani, What caused the atmosphere's CO_2 content to rise during the last 8000 years? Geochem. Geophys. Geosystems 2 (2001) 1–12 (2001GC000177).
[46] W.S. Broecker, R.F. Anderson, E. Clark, M. Fleisher, Record of seafloor $CaCO_3$ dissolution in the central equatorial Pacific, Geochem. Geophys. Geosystems 2 (2001) 1–7 (2000GC000151).
[47] S. Barker, H. Elderfield, Foraminiferal calcification response to glacial–interglacial changes in atmospheric CO_2, Science 297 (2002) 833–836.
[48] W.S. Broecker, E. Clark, Glacial-age deep sea carbonate ion concentrations, Geochem. Geophys. Geosystems 4 (2003) 1047.
[49] S. Emerson, M. Bender, Carbon fluxes at the sediment–water interface of the deep-sea: calcium carbonate preservation, J. Mar. Res. 39 (1981) 139–162.
[50] R.A. Jahnke, D.B. Craven, D.C. McCorkle, C.E. Reimers, $CaCO_3$ dissolution in California continental margin sediments: the influence of organic matter remineralization, Geochim. Cosmochim. Acta 61 (1997) 3587–3604.
[51] D. Archer, E. Maier-Reimer, Effect of deep-sea sedimentary calcite preservation on atmospheric CO_2 concentration, Nature 367 (1994) 260–263.
[52] D.M. Sigman, D.C. McCorkle, W.R. Martin, The calcite lysocline as a constraint on glacial/interglacial low-latitude production changes, Glob. Biogeochem. Cycles 12 (1998) 409–427.
[53] A. Sanyal, N.G. Hemming, G.N. Hanson, W.S. Broecker, Evidence for a higher pH in the glacial ocean from boron isotopes in foraminifera, Nature 373 (1995) 234–236.
[54] A. Sanyal, N.G. Hemming, W.S. Broecker, D.W. Lea, H.J. Spero, G.N. Hanson, Oceanic pH control on the boron isotopic composition of foraminifera: evidence from culture experiments, Paleoceanography 11 (1996) 513–517.
[55] T.M. Marchitto, W.B. Curry, D.W. Oppo, Zinc concentrations in benthic foraminifera reflect seawater chemistry, Paleoceanography 15 (2000) 299–306.
[56] D.C. McCorkle, P.A. Martin, D.W. Lea, G.P. Klinkhammer, $\delta^{13}C$, Cd/Ca, Ba/Ca, and Sr/Ca results from the Ontong Java Plateau, Paleoceanography 10 (1995) 699–714.
[57] E.A. Boyle, Cadmium: chemical tracer of deepwater paleoceanography, Paleoceanography 3 (1988) 471–489.
[58] E.A. Boyle, Y. Rosenthal, Chemical hydrography of the South Atlantic during the last glacial maximum: Cd vs. $\delta^{13}C$, in: G. Wefer, et al., (Eds.), The South Atlantic: Present and Past Circulation, Springer-Verlag, Berlin, 1996, pp. 423–443.
[59] E.A. Boyle, L.D. Keigwin, Comparison of Atlantic and Pacific paleochemical records for the last 215,000 years: changes in deep ocean circulation and chemical inventories, Earth Planet. Sci. Lett. 76 (1985/86) 135–150.
[60] E.A. Boyle, Cadmium and $\delta^{13}C$ paleochemical ocean distributions during the stage 2 glacial maximum, Annu. Rev. Earth Planet. Sci. 20 (1992) 245–287.
[61] R.G. Fairbanks, Glacio-eustatic sea level record 0–17,000 years before present: influence of glacial melting rates on Younger Dryas event and deep ocean circulation, Nature 342 (1989) 637–642.
[62] J.F. Adkins, K. McIntyre, D.P. Schrag, The salinity, temperature, and $\delta^{18}O$ of the glacial deep ocean, Science 298 (2002) 1769–1773.
[63] P.A. Martin, D.W. Lea, Y. Rosenthal, N.J. Shackleton, M. Sarnthein, T. Papenfuss, Quaternary deep sea temperature histories derived from benthic foraminiferal Mg/Ca, Earth Planet. Sci. Lett. 198 (2002) 193–209.
[64] H. Elderfield, C.J. Bertram, J. Erez, A biomineralization model for the incorporation of trace elements into foraminiferal calcium carbonate, Earth Planet. Sci. Lett. 142 (1996) 409–423.
[65] Unesco, Thermodynamics of the carbon dioxide system in seawater, Unesco Technical Papers in Marine Science 51, Paris, 1987, p. 41.
[66] K.W. Bruland, G.A. Knauer, J.H. Martin, Zinc in north–east Pacific water, Nature 271 (1978) 741–743.
[67] M. Stuiver, P.J. Reimer, E. Bard, J.W. Beck, G.S. Burr, K.A. Hughen, B. Kromer, G. McCormac, J. van der Plicht, M. Spurk, INTCAL98 radiocarbon age calibration, 24,000–0 cal BP, Radiocarbon 40 (1998) 1041–1083.
[68] R.L. Rutberg, S.R. Hemming, S.L. Goldstein, Reduced North Atlantic Deep Water flux to the glacial Southern Ocean inferred from neodymium isotope ratios, Nature 405 (2000) 935–938.
[69] A.C. Mix, N.G. Pisias, W. Rugh, A.M.J. Wilson, T. Hagelberg, Benthic foraminiferal stable isotope record from Site 849, 0–5Ma: local and global climate changes, in: L.M.N.G. Pisias, T. Jancek, A. Palmer Julson, T.H. van Andel (Eds.), Proc. ODP, Scinetific Results, vol. 138, Ocean Drilling Program, College Station TX, 1995, pp. 371–412.
[70] E.A. Boyle, Manganese carbonate overgrowths on foraminifera tests, Geochim. Cosmochim. Acta 47 (1983) 1815–1819.
[71] L.A. Mayer, et al., Site 849, in: L.A. Mayer, et al., (Eds.), Proceedings of the Ocean Drilling Program, Initial Reports Part II, vol. 138, Ocean Drilling Program, College Station, TX, 1992, pp. 735–807.
[72] F. Albarede, S.L. Goldstein, World map of Nd isotopes in sea-floor ferromanganese deposits, Geology 20 (1992) 761–763.
[73] M. Frank, N. Whiteley, S. Kasten, J.R. Hein, K. O'Nions, North Atlantic Deep Water export to the Southern Ocean over the past 14 Myr: evidence from Nd and Pb isotopes in ferromanganese crusts, Paleoceanography 17 (2002).
[74] S. Emerson, D. Archer, Glacial carbonate dissolution cycles and atmospheric pCO_2: a view from the ocean bottom, Paleoceanography 7 (1992) 319–331.
[75] D.M. Anderson, Attenuation of millennial-scale events by bioturbation in marine sediments, Paleoceanography 16 (2001) 352–357.
[76] U.S. Ninnemann, C.D. Charles, Changes in the mode of Southern Ocean circulation over the last glacial cycle revealed by foraminiferal stable isotopic variability, Earth Planet. Sci. Lett. 201 (2002) 383–396.

[77] A.J. Ridgwell, A.J. Watson, M.A. Maslin, J.O. Kaplan, Implications of coral reef buildup for the controls on atmospheric CO_2 since the Last Glacial Maximum, Paleoceanography 18 (2003) 1083.
[78] J.O. Kaplan, I.C. Prentice, W. Knorr, P.J. Valdes, Modeling the dynamics of terrestrial carbon storage since the Last Glacial Maximum, Geophys. Res. Lett. 29 (2002) 2074.
[79] D.A. Ryan, B.N. Opdyke, J.S. Jell, Holocene sediments of Wistari Reef: towards a global quantification of coral reef related neritic sedimentation in the Holocene, Palaeogeogr. Palaeoclimatol. Palaeoecol. 175 (2001) 173–184.
[80] A. Indermuhle, T.F. Stocker, F. Joos, H. Fischer, H.J. Smith, M. Wahlen, B. Deck, D. Mastroianni, J. Tschumi, T. Blunier, R. Meyer, B. Stauffer, Holocene carbon-cycle dynamics based on CO_2 trapped in ice at Taylor Dome, Antarctica, Nature 398 (1999) 121–126.
[81] M.A. Maslin, E. Thomas, Balancing the deglacial global carbon budget: the hydrate factor, Quat. Sci. Rev. 22 (2003) 1729–1736.
[82] T. Crowley, Ice age terrestrial carbon changes revisited, Glob. Biogeochem. Cycles 9 (1995) 377–390.
[83] J.M. Adams, H. Faure, A new estimate of changing carbon storage on land since the last glacial maximum, based on global land ecosystem reconstruction, Glob. Planet. Change 16–17 (1998) 2–24.
[84] P. Loubere, A multiproxy reconstruction of biological productivity and oceanography in the eastern equatorial Pacific for the past 30,000 years, Mar. Micropaleontol. 37 (1999) 173–198.
[85] J.P. Kennett, K.G. Cannariato, I.L. Hendy, R.J. Behl, Carbon isotopic evidence for methane hydrate instability during Quaternary interstadials, Science 288 (2000) 128–133.
[86] H.J. Spero, D.W. Lea, The cause of carbon isotope minimum events on glacial terminations, Science 296 (2002) 522–525.
[87] A.M. Shiller, E.A. Boyle, Dissolved zinc in rivers, Nature 317 (1985) 49–52.
[88] R.A. Duce, et al., The atmospheric input of trace species to the world ocean, Glob. Biogeochem. Cycles 5 (1991) 193–259.
[89] J.M. Edmond, A.C. Campbell, M.R. Palmer, G.P. Klinkhammer, C.R. German, H.N. Edmonds, H. Elderfield, G. Thompson, P. Rona, Time series studies of vent fluids from the TAG and MARK sites (1986, 1990) Mid-Atlantic Ridge: a new solution chemistry model and a mechanism for Cu/Zn zonation in massive sulphide orebodies, in: L.M. Parson, C.L. Walker, D.R. Dixon (Eds.), Hydrothermal Vents and Processes, Geological Society Special Publication, vol. 87, 1995, pp. 77–86.
[90] J.H. Martin, A.J. Thomas, The global insignificance of telluric input of dissolved trace metals (Cd, Cu, Ni and Zn) to ocean margins, Mar. Chem. 46 (1994) 165–178.
[91] A. Indermuhle, E. Monnin, B. Stauffer, T.F. Stocker, M. Wahlen, Atmospheric CO_2 concentration from 60 to 20 kyr BP from the Taylor Dome ice core, Antarctica, Geophys. Res. Lett. 27 (2000) 735–738.
[92] H.J. Smith, H. Fischer, M. Wahlen, D. Mastroianni, B. Deck, Dual modes of the carbon cycle since the Last Glacial Maximum, Nature 400 (1999) 248–250.